

Study on sintering kinetics and activation energy of UO_2 pellets using three different methods

D. Lahiri, S.V. Ramana Rao *, G.V.S. Hemantha Rao, R.K. Srivastava

Characterization Laboratory, Nuclear Fuel Complex, Hyderabad 500061, India

Received 7 December 2005; accepted 22 May 2006

Abstract

During early stages of sintering of UO_2 , diffusion of metallic ions plays the vital role as this is the rate controlling step of the sintering at that stage. Sintering kinetics and the activation energy at the early stages of sintering of UO_2 in reducing atmosphere has been studied by several workers using different methods of calculation. The diffusion mechanisms that have been found to operate at this stage are grain boundary diffusion and volume diffusion. The activation energy calculated by different studies also varies widely. In the following study, sintering mechanism and activation energy for sintering of UO_2 in reducing atmosphere has been studied by three different methods, namely, rate controlled sintering, constant heating rate and Dorn's method. The kinetics of sintering and activation energy has been found to change with temperature. Initially grain boundary diffusion operates and in the later stage volume diffusion controls. Calculation of activation energy by the above methods shows that the rate controlled sintering and constant heating rate produces similar results, whereas the results of Dorn's method are not quite matching.

© 2006 Elsevier B.V. All rights reserved.

1. Introduction

In most of the light and heavy water thermal reactors uranium dioxide (UO_2) is used as fuel material. The acceptance of UO_2 for this application is mainly because of its high melting point, good dimensional and radiation stability and its excellent chemical compatibility with other components of the reactor. Its main disadvantages are its low thermal conductivity and low fissile atom density that results into high centerline temperature and large volume pores.

Uranium dioxide fuel pellets are sintered in reducing atmospheres with the aim of achieving a final O/U ratio of around 2.00 [1]. Pellets are produced through powder metallurgical route i.e., by milling, pre-compaction, granulation, cold compaction and high temperature sintering performed in a sequence. The sintering process is diffusion controlled one, whose rate is controlled by the slower moving metal atoms. Uranium diffusion at grain boundaries controls the initial stages of uranium dioxide sintering. [1,2]. The sintering kinetics of UO_2 during initial stages have been studied by several workers. Lay and Carter [3] have found out the sintering mechanism to be volume diffusion of uranium ion, whereas Bacmann and Cizeron [4] and Woolfrey [5] have suggested that to be grain boundary diffusion. The

* Corresponding author. Tel.: +91 40 27184032; fax: +91 40 27121209.

E-mail address: svrr@nfc.ernet.in (S.V. Ramana Rao).

activation energies for initial stages of sintering, reported by different workers varies in a wide range from 84 kJ/mol [6] to 420 kJ/mol [7].

To know the kinetics of sintering and to calculate the activation energy of the process two different methods are employed that uses dilatometer data of dimensional change with respect to temperature and time. The two different types of methods used for several studies are (1) isothermal methods, e.g., rate controlled sintering (RCS) method used by Kutty et al. [8], and (2) non-isothermal methods, e.g., Dorn's method [2,7] and constant heating rate method [2]. Rate controlled sintering method is a more accurate one, whereas the other two are approximate ones but very easy and fast for calculation purpose.

The main objective of this study is to find out the sintering kinetics and activation energy of UO_2 pellets and to compare the results calculated by the three methods.

2. Theory

2.1. Rate controlled sintering

In this method a special type of sintering schedule is adopted in which some threshold value of shrinkage rate is fixed during the process. Initially, the green pellet is heated in a dilatometer at a constant heating rate defined for the process until the shrinkage rate (dl/dt) exceeds the threshold value. At this stage the temperature rise is stopped and shrinkage now takes place in isothermal conditions. Once the shrinkage rate comes below the threshold value temperature again starts rising. The experimental shrinkage curve obtained by dilatometry is generally in the form [9]:

$$\Delta l/l_0 = y = [K(T)t]^n, \quad (1)$$

where l_0 is the initial length of the green pellet at the starting stage of sintering, $K(T)$ is the Arrhenius constant, t is the time and n is a constant whose value depends on the sintering mechanism. If only the volume diffusion is operative, then the shrinkage rate is given by

$$dy/dt = n(5.34\gamma\Omega D_v/kTa^3)^n t^{n-1}, \quad (2)$$

where $n = 0.49$.

Similarly, for grain boundary diffusion alone

$$dy/dt = n(2.14\gamma\Omega bD_b/kTa^4)^n t^{n-1}, \quad (3)$$

where $n = 0.33$. where γ is the surface tension, Ω is the vacancy volume, D_v and D_b are the diffusion coefficients for volume and grain boundary diffusions respectively. T is the temperature, a is the particle radius, b is the thickness of grain boundary and k is the Boltzmann constant. The slope of the plot of $\log dy/dt$ vs $\log t$ will be $(n - 1)$ from which the sintering exponent can be evaluated. From the value of the intercepts, the diffusion coefficient could be evaluated. The variation of D with temperature is defined as

$$D = D_0 \exp(-Q/RT), \quad (4)$$

where D_0 is the pre-exponential factor, Q is the activation energy and R is the molar gas constant. The slope of the plot of $\log D$ and $\log(1/T)$ gives the $-Q/R$. R being a constant of value $8.31441 \text{ J K}^{-1} \text{ mol}^{-1}$, Q is determined from the slope of the plot.

2.2. Dorn's method

This method, initially proposed by Dorn [10] for studying creep, gives a very fast and direct access to the measurement of activation energy. The isothermal shrinkage rate $v_1 = dy/dt$ is at first recorded at a temperature T_1 for a sintering time t . Then, following a temperature increment made as quickly as possible, the same recording is made at a temperature T_2 , temperature interval being not very high. The shrinkage rate in this interval is recorded to be v_2 .

Eq. (1) can also be written in the form

$$y^m = (\Delta l/l_0)^m = K(T)t, \quad (5)$$

where $m = 1/n$ and

$$K(T) = (AD_0\Omega\gamma/G^{zk})\{\exp(-Q/RT)/T\}, \quad (6)$$

where γ is the free surface energy, Ω is the atomic volume, G is the size of the crystallite, k is the Boltzmann's constant, D_0 is the pre-exponential term of the diffusion coefficient, m , α and A are constants dependant on the geometric shape chosen for the particles. Eq. (5) in differential form is

$$dy/dt = K(T)y^{1-m}/m. \quad (7)$$

Assuming the microstructural state remains unchanged during the temperature increment, we have the relation,

$$(\Delta l/l_0)_{\text{end step 1}} = (\Delta l/l_0)_{\text{beginning step 2}}, \quad (8)$$

implying this for the shrinkage rate, we get,

$$v_2/v_1 = (T_1/T_2) \exp[(-Q/R)(1/T_2 - 1/T_1)] \quad (9)$$

The equation for calculation of activation energy, deduced from Eq. (9) is of the form:

$$Q = \{RT_2T_1/(T_2 - T_1)\} \ln(T_2v_2/T_1v_1). \quad (10)$$

The assumption for this model is that the microstructural state remains unchanged during the temperature increment, which may not be true at high densification levels.

2.3. Constant heating rate method

This method, proposed by Wang and Raj [11] is very simple to formulate. Using Eqs. (5) and (6) the relative shrinkage rate could be written as,

$$dy/dt = \{k_0f(y) \exp(-Q/RT)\}/G^{zk}T, \quad (11)$$

where $f(y) = y^{1-m}/m$ and $k_0 = AD_0\Omega\gamma$.

In the constant heating rate method, where the constant heating rate is $a = dT/dt$, the relative shrinkage rate may be written as

$$dy/dt = a(dy/dT). \quad (12)$$

By substituting Eq. (12) in Eq. (11) and taking logarithm on both the sides, we can get the following equation:

$$\ln\{Ta(dy/dT)\} = -Q/RT + \ln k_0 - \ln G^{zk} + \ln\{f(y)\}. \quad (13)$$

Plotting $\ln\{Ta(dy/dT)\}$ as a function of $1/T$ gives the value of Q/R as the slope of the plot, assuming other terms to be constant.

3. Experimental procedure

The UO_2 powder used in this study is produced by ADU route. Characterization of the powder is performed as per the specification, the relevant data used in further calculation of activation energy are given in Table 1. After characterization, powder is granulated and compacted into green pellets of 20 mm diameter and 30 mm height. Organic binders were used for pelletization. All the process parameters for the pellets used in this

Table 1
Characterization of UO_2 powder

| | |
|---|-----------------------|
| Oxygen to metal ratio | 2.00 |
| Theoretical density (g m ³) | 10.96×10^6 |
| Free surface energy, γ (J/m ²) | 0.6 |
| Particle radius ^a , a (m) | 4.47×10^{-8} |
| Specific surface area, s (m ² /gm) | 3.06 |

^a $a = 6/(2\rho sf)$, where f is the shape factor.

study are exactly same. Sintering was performed in a vertical high temperature dilatometer supplied by M/s Anter Corporation and the model is 1161™. All the sintering tests were performed in reducing atmosphere of $N_2 + H_2$ (5% by volume). For the rate controlled sintering study, the threshold shrinkage rate was controlled at $12 \mu/s$. The heating rate was 5 K/min up to 1973 K and then cooling. For the Dorn's method, the temperature increment was given at a step of 30 K in 1 min in a temperature range of 1173–1443 K in 10 steps, and at each step a soaking of 30 min has been given. For constant heating rate method, the heating rate was 1 K/min.

Time vs. dimensional shrinkage plots are obtained from dilatometric studies for all the pellets. Data obtained thus were analysed using different methods as mentioned above to find out the kinetics of sintering and the activation energy of the UO_2 pellets. The green density of the pellets has been calculated by geometrical method and the sintered density by Archimedes principle.

The fractured surface of the pellets was observed under scanning electron microscope of Philips XL30 model operating at 20 kV for microstructural studies.

4. Results

Fig. 1 shows the variation of the shrinkage rate occurring at each isothermal step during sintering. It is observed that the first isothermal sintering step is at 1223 K and at each increase of 50 K temp, isothermal sintering is taking place. The sintering in this method is controlled by specified shrinkage rate. Fig. 2 gives the plots of $\log(dy/dt)$ vs. $\log(t)$

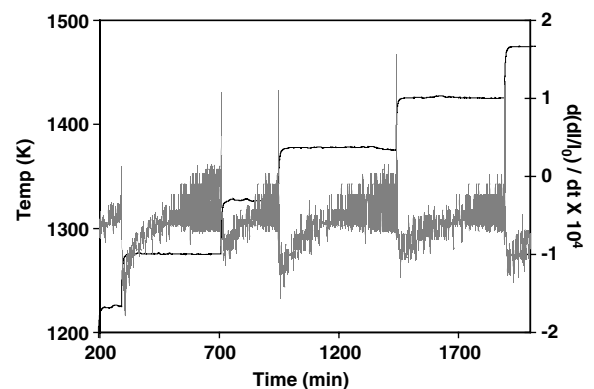


Fig. 1. RCS showing the variation in dy/dt occurring in each isothermal step.

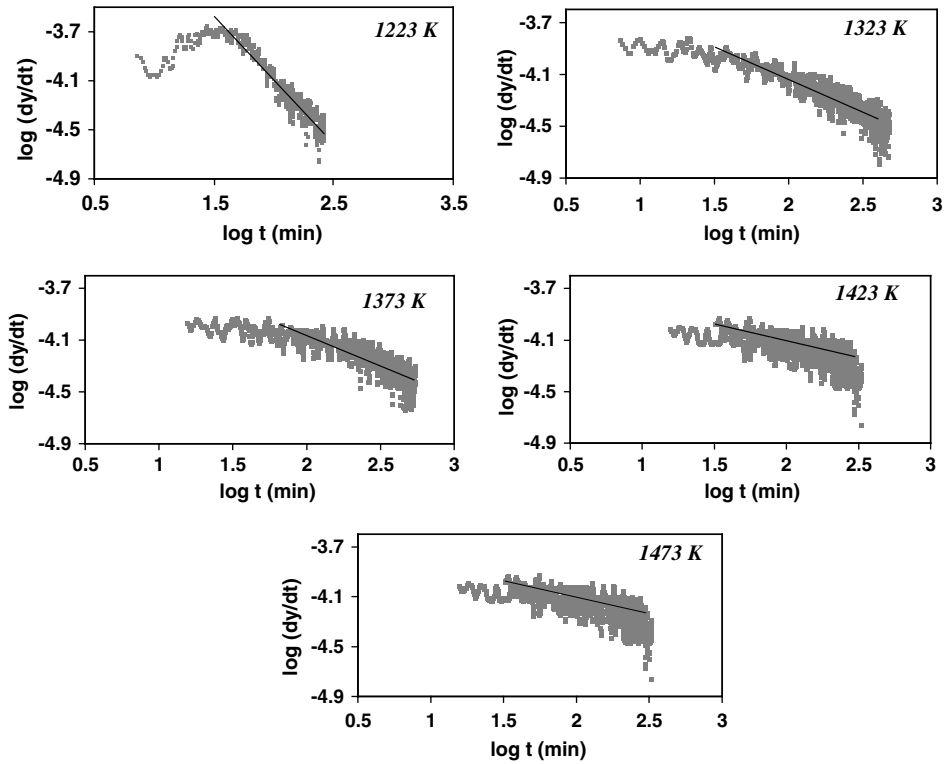


Fig. 2. Plots of $\log(dy/dt)$ vs. $\log t$ for the pellet used in RCS study for different temperatures as mentioned in the plots. The slope of the curves will be $(n - 1)$ from which the sintering exponent ‘ n ’ can be evaluated.

at different isothermal steps. From the slope of the plots, the sintering exponent ‘ n ’ has been determined for each isothermal temperature step. The value of ‘ n ’ varies from 0.33 at 1223 K to 0.67 at 1473 K (Table 2). From the values of ‘ n ’, it is evident that at the temperature of 1223 K, grain boundary diffusion is the rate controlling mechanism. But, from the next step, i.e., 1323 K onwards volume diffusion plays the major role. Fig. 3 is the Arrhenius plot of $\ln D$ vs $1/T$. The slope of the plot in Fig. 3 gives the activation energy Q (Table 2). The activation energy is calculated as per Eq. (4) is 287 kJ/mole, which is matching with previous studies (7).

Table 2
Activation energies calculated in rate controlled sintering

| Sample ID | Temperature (K) | ‘ n ’ value | Activation energy (kJ/mol) |
|-----------|-----------------|---------------|----------------------------|
| S1 | 1223 | 0.33 | 287 |
| | 1323 | 0.49 | |
| | 1373 | 0.53 | |
| | 1423 | 0.64 | |
| | 1473 | 0.67 | |

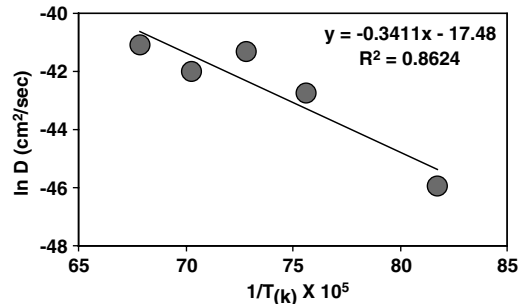


Fig. 3. The Arrhenius plot $\ln D$ vs. $1/T$ for the pellet used in RCS study. The slope of the plot is $-Q/R$. R being a constant of value $8.31441 \text{ J K}^{-1} \text{ mol}^{-1}$, Q is calculated from the slope of the plot.

Fig. 4 shows the shrinkage curve of the pellet sintered with constant heating rate of 1 K/min which shows the onset of shrinkage at around 1173 K. Fig. 5 is the plot $\ln\{T\alpha(dy/dT)\}$ as a function of $1/T$. The slope gives the value of Q/R from which the activation energy can be calculated. Table 3 gives the activation energy calculated at 50 K interval between 1223 K and 1473 K. Initially the activation energy is very high at 1223 K, but then drastically changes to a lower value with an increase

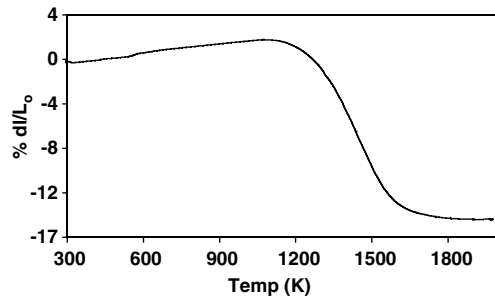


Fig. 4. Plot of % shrinkage with temperature for pellet S2 sintered using Constant heating rate method.

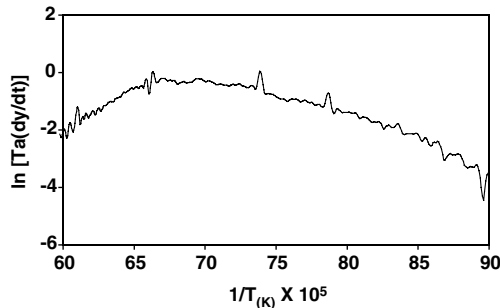


Fig. 5. Plot for calculation of Q using constant heating rate method.

Table 3
Activation energies calculated in constant heating rate method

| Sample ID | Temperature range (K) | Activation energy (kJ/mol) |
|-----------|-----------------------|----------------------------|
| S2 | 1173–1223 | 257 |
| | 1223–1273 | 138 |
| | 1273–1373 | 108 |
| | 1373–1473 | 78 |

of temperature by 50 K and with further increase in temperature the change is minimal. Fig. 6 is the plot of activation energy with increasing temperature, as calculated by constant heating rate method, which shows that the activation energy decreases drastically with increase in temperature initially.

Table 4 reports the activation energy calculated by Dorn's method using Eq. (10) for each temperature step at an interval 30 K from 1203 K to 1443 K. Fig. 7 is, the plot of activation energy with increasing temperature, but drawn from the values calculated by Dorn's method. This plot also shows the same trend as constant heating rate method. Table 5 gives the sintered density and O/U ratio

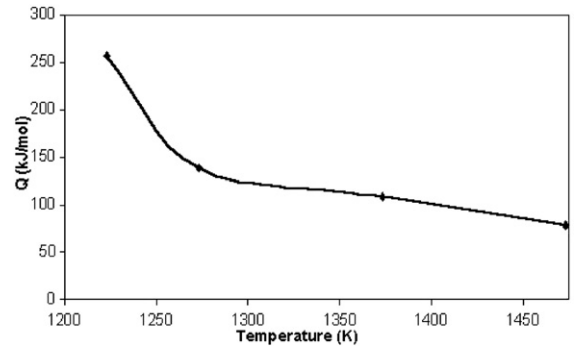


Fig. 6. Change in Q values with increasing temperature observed for constant heating rate method.

Table 4
Activation energies calculated by Dorn's method

| T_1 (K) | T_2 (K) | Activation energy (kJ/mol) |
|-----------|-----------|----------------------------|
| 1203 | 1233 | 187 |
| 1233 | 1263 | 88 |
| 1263 | 1293 | 93 |
| 1293 | 1323 | 88 |
| 1323 | 1353 | 90 |
| 1353 | 1383 | 83 |
| 1383 | 1413 | 73 |
| 1413 | 1443 | 81 |
| 1443 | 1473 | 94 |

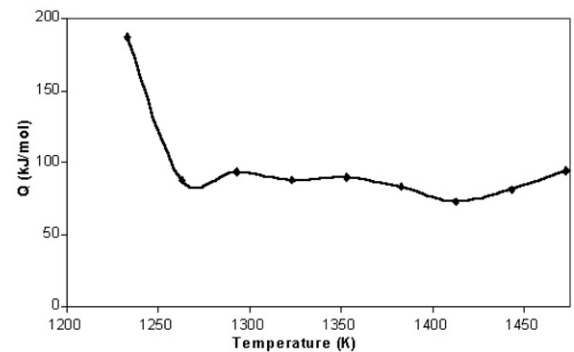


Fig. 7. Change in Q values with increasing temperature observed for Dorn's method.

Table 5
Property of the sintered pellets

| Sample ID | Sintered density (%TD) | O/U Ratio |
|-----------|------------------------|-----------|
| S1 | 96.8 | 2.00 |
| S2 | 96.5 | 2.00 |
| S3 | 96.8 | 2.00 |

of the sintered pellets. Sintered densities for all the pellets are quite similar and same trend is followed for O/U ratio also.

Figs. 8 and 9 show the scanning electron micrographs of the UO_2 pellets during sintering at 1223 K and 1373 K respectively. The former one shows small particles with interconnected porosities, whereas the later one is having large particles with isolated porosities. The two micrographs show clearly the vast difference in the microstructural aspects of this two stages of sintering. In case of Dorn's method, the incremental step is as high as

30 K. So, with only five steps, a lot of change in microstructure has taken place. That is why the basic assumption of Dorn's method, i.e., the microstructural state remains unchanged during the temperature increment does not hold good for the present study. Hence, the calculation made by Dorn's method may not be a true representation of sintering mechanism and activation energy for this study.

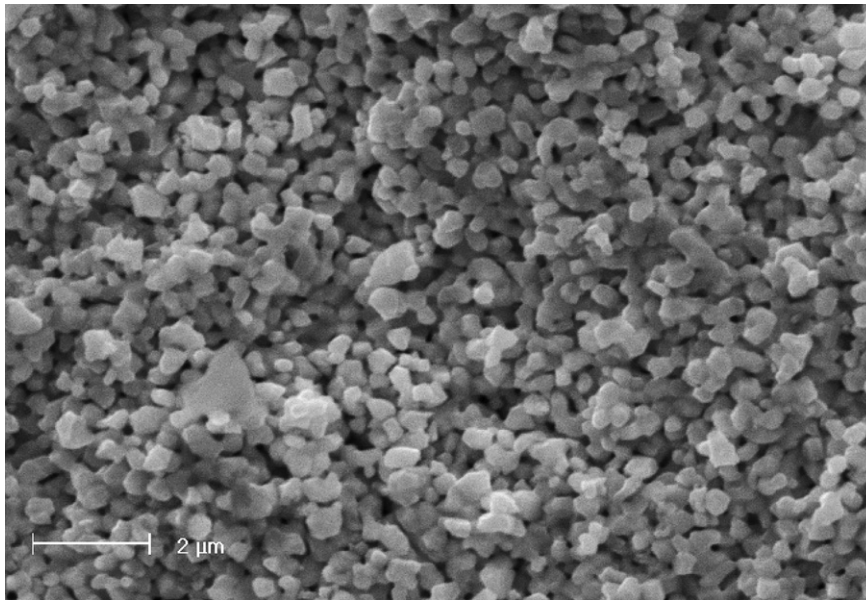


Fig. 8. Scanning electron micrograph of fractured surface for the pellet sintered at 1223 K.

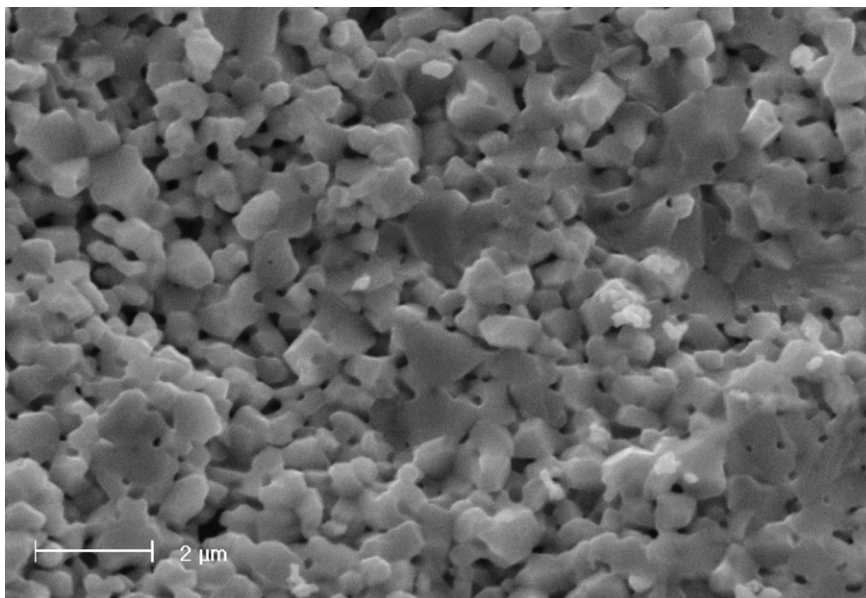


Fig. 9. Scanning electron micrograph of fractured surface for the pellet sintered at 1373 K.

5. Discussion

Sintering provides the inter particle bonding that generates the attractive forces needed to hold together the otherwise loose ceramic powder mass. Particles sinter together by atomic motions that act to eliminate the high surface energy associated with unsintered powder. However, not all of the surface energy is necessarily available as driving force for sintering, the grain boundaries prove to be important to atomic motion because the boundaries are defective regions with high atomic mobility. Grain boundary diffusion is fairly important to densification for most crystalline materials and appears to dominate the densification of many common ceramics.

In case of normal sintering in reducing atmosphere with a heating rate of 1 K/min, shrinkage starts at around 1173 K. Maximum shrinkage rate is observed at around 1523 K. Sintering of oxide fuel should be done with an oxygen potential in the range of -126 to -504 kJ/mol, typical of dry hydrogen [12,13]. In the case of the present study, the sintering gas used is having an oxygen concentration of <5 ppm, which ensures a highly reducing sintering atmosphere. All the pellets sintered in this study are analysed for the O/U ratio and all are found to be perfectly stoichiometric (Table 5). This means that they have a low defect concentrations. Since the concentration of defects in these pellets are low, the driving force for sintering is also very small. That is why they require sintering at temperatures as high as 1973 K for getting good sintered densities.

As per Kutty et al. [1], at the stoichiometric composition, the concentration of uranium vacancies is higher than that of uranium interstitials. Hence, the vacancy mechanism is likely to operate during sintering of the pellets in this study. In case of early stage of sintering, the diffusion of metallic ions is the slowest step and hence, is the rate controlling mechanism for sintering. Therefore, during the early stages of sintering diffusion mechanism is a very important phenomenon. In the RCS method the 'n' values found from the slope of the $\log(dy/dt)$ vs. $\log(t)$ plot at different isothermal steps (Fig. 2) gives the idea of the diffusion mechanisms operating at those stages of sintering. From the values of 'n' (Tables 2), it is evident that at the isothermal step of 1223 K, grain boundary diffusion is the rate controlling mechanism. This observation can be supported by the basic requirements of grain

boundary diffusion and volume diffusion mechanisms. Volume diffusion is prevalent with very high temperature sintering of large particles. Grain boundary diffusion is usually dominant with smaller particle size. Small particles exhibit faster neck growth and need less sintering time or a lower sintering temperature to achieve an equivalent degree of sintering. Generally, large particles will sinter slower and acquire higher sintering temperature or longer sintering times to attain an equivalent degree of densification. In the present study, initially at lower sintering temperature of around 1173–1223 K, at the onset of sintering, the particles are smaller in size with interconnected porosities present. This is the ideal condition for grain boundary diffusion to take place. So, faster neck growth takes place. As the necks grow enough and big particles are produced by coalescence as the temperature increases, its now the volume diffusion mechanism that takes the control of the sintering process.

SEM micrographs presented in Figs. 8 and 9 also support the facts as stated above. Micrograph of the pellet at 1223 K (Fig. 8) shows small particles with necks being formed between them and interconnected porosities all around. Fig. 9 of the pellet at 1373 K shows large particles (grains) with isolated porosities present in between. From the activation energy point of view also, there is a drastic change between the energy values in the range of 1173–1223 K and above 1223 K, beyond which, the change is very low with respect to temperature in case of both constant heating rate method and Dorn's method for activation energy calculation (Tables 3 and 4). This clearly indicates the change of diffusion kinetics in the range of around 1223–1273 K. RCS method, constant heating rate method and Dorn's method have been used for activation energy calculation for the present study. In case of RCS method, the activation energy is calculated using all the diffusion coefficients, for five isothermal sintering steps in the temperature range of 1223–1473 K. For constant heating rate method, the activation energy is calculated at 1223 K and for every 50 K step up to temperature 1473 K. For Dorn's method, the activation energy has been determined for each incremental step of 30 K starting from 1203 K up to 1473 K.

Activation energy found by RCS method is 287 kJ/mol. For the constant heating rate, in the initial stages of sintering, the activation energy is as high as 257 kJ/mol, which is quite matching with the value calculated by RCS method. But, at higher

temperatures, in the region of volume diffusion, the activation energy value drastically changes to a lower value of 138 kJ/mol and afterwards the changes are minimal (Table 3). For a temperature range of 200 K, the activation energy value ranges between 80 and 140 kJ/mol. In the case of Dorn's method also the trend is same, i.e., initially the activation energy value is very high at around 1223 K and then drastically falls to a very low value within a temperature range of 50 K and then it becomes almost constant (Table 4). This trend clearly indicates the changeover of the diffusion mechanism in the temperature region of 1223–1273 K. Though, the trend of activation energy variation with increasing temperature is same in case of both constant heating rate method and Dorn's method, but the actual values calculated in Dorn's method are much lower than the other ones. The highest activation energy calculated in case of Dorn's method is 187 kJ/mol, which changes drastically to <100 kJ/mol in the next temperature increment.

RCS method is the most preferred one amongst all three methods. Constant heating rate could also be used as a rough estimate. In the case of the present study, activation energy values calculated by RCS method and constant heating rate method are in good agreement. Dorn's method [10] has basically been developed for creep study, though it has been used in several studies on sintering kinetics [2,7]. But, in case of the present study, the calculations made using Dorn's method are not quite satisfactory and hence the method has been found not as suitable or perfect as the other two for study of the sintering kinetics of UO_2 powder.

Another important observation from the present study is that the exponent ' n ' for sintering and activation energy ' Q ' is changing with increasing temperature (Tables 2 and 3). Hence, ' n ' and ' Q ' could not be taken as constant during calculations made by RCS, constant heating rate and Dorn's method. In this context, the adequacy of those methods for using in the present study comes into picture. Dorn's method is, anyway, not suitable because of its basic assumption regarding no change in microstructure during sintering which is not valid in this case. In the case of RCS method, exponent ' n ' is determined separately for each isothermal step. So, during ' n ' calculation there is no change of temperature. Hence, ' n ' could be calculated correctly with RCS method and different diffusion mechanisms operating at each isothermal steps could be predicted correctly. But, for determination of ' Q '

it uses Eq. (4), where ' Q ' is assumed to be constant with respect to temperature and it is calculated from the slope of a plot between diffusion coefficients and temperature. Hence, calculation of ' Q ' in this way is not correct for all the cases, for example, in the case of the present study. If ' Q ' value is same throughout a sintering process, then only ' Q ' could be determined by this method.

Otherwise, ' Q ' has to be taken as a function of temperature and then some method has to be developed to find out the same at different temperature levels throughout the process at each of the isothermal steps. For constant heating rate method also the same argument is valid, i.e., ' Q ' is taken to be constant while determining it from the slope of the plot obtained from Eq. (13), which is not true. But, there is some flexibility in case of constant heating rate method. Here, ' Q ' could be determined for any temperature range required, no matter how long or how short it is. By taking small ranges in temperature, gradual change in ' Q ' could be determined and at the same time range of temperature could be found out in which the ' Q ' is almost constant. Then, ' Q ' vs. ' T ' plot could be drawn from which ' Q ' at any temperature could be predicted.

6. Conclusions

It has been found in the present study on sintering kinetics of UO_2 pellets that, while sintering in reducing atmosphere, initially at lower temperatures grain boundary diffusion takes place. With increase in temperature volume diffusion becomes active.

It has also been noticed that pellet microstructure during sintering plays a significant role on the diffusion mechanism. At lower temperature, with smaller particles and interconnected porosities, grain boundary diffusion is prevalent. Whereas with increase in temperature, as particles becomes coarser and pores are isolated, volume diffusion dominates the sintering process.

Activation energy is high in the initial stage of sintering and then it drastically falls to a lower value above 1223 K, afterwards does not vary much.

Activation energy values calculated by RCS method and constant heating rate method are in good agreement, but Dorn's method gives the values in a significantly lower range. Moreover, Dorn's method is not suitable because of its basic assumption regarding the unchanged microstructural state during sintering which is not valid always. Diffusion

mechanism could be predicted correctly with RCS method but some method has to be developed taking ' Q ' as a function of temperature to find out the activation energy throughout the process. In the constant heating rate method gradual change in ' Q ' could be determined taking small temperature ranges into calculation. And activation energy at any temperature could be predicted from the ' Q ' vs. ' T ' plot.

Acknowledgements

Authors acknowledge the valuable help of Dr C. Padmaprabu, Scientific Officer, Characterization Lab, NFC for the SEM study of pellet microstructure. Authors are also grateful to Shri. R.N. Jayaraj, Chief Executive, NFC for his encouragement during the study.

References

- [1] T.R.G. Kutty, P.V. Hegde, K.B. Khan, U. Basak, S.N. Pillai, A.K. Sengupta, G.C. Jain, S. Majumdar, H.S. kamath, D.S.C. Purushotham, *J. Nucl. Mater.* 305 (2002) 159.
- [2] Ph. Dehault, L. Bourgeois, H. Chevrel, *J. Nucl. Mater.* 299 (2001) 250.
- [3] K.W. Lay, R.E. Carter, *J. Nucl. Mater.* 30 (1969) 74.
- [4] J.J. Bacmann, G. Cizeron, *J. Nucl. Mater.* 33 (1969) 271.
- [5] J.L. Woolfrey, *J. Am. Ceram. Soc.* 55 (1972) 383.
- [6] M.M. Ristic, E. Kostic, NP-14124 (1963).
- [7] J.J. Bacmann, G. Cizeron, *J. Am. Ceram. Soc.* 51 (1968) 209.
- [8] T.R.G. Kutty, K.B. Khan, P.V. Hegde, A.K. Sengupta, S. Majumdar, D.S.C. Purushotham, *J. Nucl. Mater.* 297 (2001) 120.
- [9] D.L. Johnson, *J. Appl. Phys.* 40 (1969) 192.
- [10] J.E. Dorn, in: R. Maddin (Ed.), *Creep and Recovery*, American Society for Metals, Cleveland, OH, 1957, p. 255.
- [11] J. Wang, R. Raj, *J. Am. Ceram. Soc.* 73 (1990) 1172.
- [12] HJ. Matzke, *Philos. Mag.* 64A (1991) 1181.
- [13] D. Glasser-Leme, HJ. Matzke, *Solid State Ion.* 12 (1984) 217.